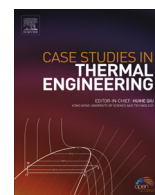


Contents lists available at ScienceDirect

Case Studies in Thermal Engineering

journal homepage: www.elsevier.com/locate/csite

A practical method for in-situ thermal characterization of walls

**Emilio Sassine***Lebanese University, Beirut, Lebanon*

ARTICLE INFO

Article history:

Received 11 February 2016

Received in revised form

18 March 2016

Accepted 22 March 2016

Available online 24 March 2016

Keywords:

Thermal characterization

Existing buildings

Heat transfer matrix

Stochastic regime

ABSTRACT

A practical and fast method for thermal characterization of walls based on complex Fourier analysis is proposed to determine the thermal capacitance (defined as the product of density and specific capacity) and the thermal conductivity for a building wall using the monitored inner/outer surface temperatures and outer heat flux. This method is useful for in-situ determination of walls' thermal properties in stochastic regimes and therefore does not require any particular constraints in boundary condition.

The minimum measurement duration was analyzed by determining the relative deviation between consecutive optimal values for R and C in order to reduce as much as possible the monitoring duration for energy auditors without losing accuracy.

© 2016 Published by Elsevier Ltd.

1. Introduction

1.1. Importance of thermal properties for energy simulation

Evaluating how much heat is lost through external walls is a key requirement for building energy simulators and is necessary for quality assurance and successful decision making in policy implementation and building design, construction and refurbishment. Nowadays energy audits constitute one of the best solutions to assess the energy consumption in existing buildings and to recommend energy efficiency measures in order to reach a better energy performance [1]. The thermal performance is generally estimated by using dynamic thermal simulations or steady state estimations using the degree-days method [2]. One of the most experienced locks in thermal modeling of buildings, whether in dynamic or even steady state conditions, is the determination of the thermal properties of walls, especially in existing buildings.

Energy auditors often use assumptions, sometimes aberrant, to overcome this problematic situation. In fact, new building components are usually certified and their physical characteristics can be specified in many cases, but when dealing with existing buildings the situation is more complicated since the properties are usually unknown, components have often been degraded during the time, and the tests should be easy, quick, and non-destructive.

1.2. Lab conditions

In the laboratory, steady state conditions can be easily imposed to any building component and then its thermal properties could be determined without major impediments [3–7].

Hadded, et al. [3] used a sample holder in copper placed between two boxes (A) and (B) for thermo physical

E-mail address: Emilio.sassine@gmail.com

<http://dx.doi.org/10.1016/j.csite.2016.03.006>

2214-157X/© 2016 Published by Elsevier Ltd.

Nomenclature		p_1, p_2, p_3, p_4 constants (–).	
φ	heat flux (W/m^2).	Subscripts	
T	temperature ($^{\circ}C$).		
R	equivalent thermal resistance (m^2K/W).	w	wall.
C	equivalent thermal capacitance (J/m^3K).	i	inner surface.
p	Laplace transform variable (–).	o	outer surface.
A, B, C, D, E, F	constants (–).	k	temperature index number.
a, b, c, d	constants (–).	cn	cosine, order n.
$\alpha, \beta, \gamma, \varepsilon, \mu$	constants (–).	sn	sine, order n.
W_{ij}	transfer matrix elements of the wall.	cte	constant.
n	harmonic index number (–).	approx	Fourier approximated.
N	harmonic order number (–).	meas	measured.
ω, Ω	angular frequency (1/s).	theo	theoretical.
D	data logging duration.		
F(p)	Laplace transform function.		

characterization of recycled textile materials used for building insulating. An electronic ohmmeter is used to measure the heat resistance (R), in order to evaluate the amount of heat produced in the system by joule effect. The same setup was used to determine the thermal conductivity and diffusivity. Fgaier, et al. [4] used the heat flow meter method to determine the dynamic thermal performance of three types of unfired earth bricks. The method consists of simultaneously measuring the heat flow and temperature on both faces of a sample subjected to a temperature gradient generated by two exchanger plates. The sample and flow meters assembly is surrounded by an insulating belt so as to limit the lateral heat flow losses and ensure a unidirectional flow in the central measurement area. Zhu, et al. [5] used the same method to determine thermal properties of recycled concrete blocks. Laaroussi, et al. [6] applied the steady state, hot plate method to estimate the thermal conductivity. The method is based on temperature measurements at the center of heating element inserted between the sample and polyethylene foam. The thermal diffusivity measurement is based on the flash method. An energy pulse heats one side of a plane-parallel sample and the transient temperature rise $T(t)$ on the backside due to the energy input is recorded. Derbal, et al. [7] presented a method to identify the thermo physical properties of a given material inserted between two layers of material for which the following characteristics are known: thermal conductivity and volumetric heat capacity. The material is subjected to a unidirectional heat flux produced by a flat heating resistance.

However, one of the disadvantages of measuring the thermal properties under a laboratory-controlled climate is that the tested specimen would then be placed within a natural actual climate which differs from the testing conditions. In addition, when dealing with existing buildings, imposing boundary conditions is usually expensive and cumbersome and is often modified by natural stochastic conditions (wind, rain, sunlight, etc ...).

1.3. In-situ measurements

Accordingly, some researchers began seeking a derivation for the thermal properties based upon in-situ measurements such as surface temperatures and heat fluxes.

Chaffar, et al. [8] used a flat heating resistance surface measuring $0.9\text{ m} \times 1.1\text{ m}$ pressed against the panel by an 18 cm thickness polystyrene panel to direct most of the power dissipated by the resistance into the wall being tested. The method consists of thermally examining an access surface by applying a heat flux and studying the response in terms of the temperature recorded by infrared thermography on the opposite surface. Although it is only necessary to record the transient temperature variation history for the transient plane source (TPS) method, it is still classified as a laboratory controlled climate as the TPS element requires heating.

Even though the method is simple and gives satisfactory results, the equipment used is still expensive and cumbersome. Outdoor test cells have been developed in order to tackle the challenging issue of experimentally characterizing innovative envelope elements in real dynamic weather conditions [9]. Awad, et al. [10] Evaluated the thermal performance of a mid-rise wood-frame building using a $3\text{ m} \times 6\text{ m}$ test house using a total of 41 sensors are installed inside the test house (24 thermocouple sensors, 10 heat flux sensors, and 7 relative humidity sensors).

However, although these methods very interesting for new envelope elements, they are not suitable to characterize existing buildings.

Some works used light equipment to evaluate thermal resistance of buildings, but they neglected the thermal capacitance which is a very important parameter for dynamic modeling. Asdrubali, et al. [11] presented the results of a measurement campaign of in situ thermal transmittance, performed in some buildings in the Umbria Region (Italy), in order to compare in situ thermal transmittance measurements and theoretical calculated U-values. Ficco, et al. [12] also presented the results of an experimental campaign and compared in situ U-values with the estimated ones from design data and field

analyses. Meng, et al. [13] determined the combined influence of the location of thermocouples and heat flow meters, the size, shape and pasting angle of the heat flow meters on the measurement accuracy of the wall heat transfer coefficient (U -value) using the heat flow meter method. Ahmad, et al. [14] conducted a study to determine the in situ thermal transmittance and thermal resistance of two exterior reinforced precast concrete walls of a building constructed with hollow panels using heat flux sensors, air temperature sensors, and thermocouples.

Luo, et al. [15] used the finite volume scheme and complex Fourier analysis methods to determine the thermal capacitance (defined as the product of density and specific capacity) and thermal conductivity for a building construction layer using the monitored inner/outer surface temperatures and heat fluxes. The instrumentation recorded the external weather conditions; wind speed and direction, air temperature, relative humidity and, the incident solar radiation on each wall (vertical plane) and the horizontal plane. For each module, temperature and heat flux profiles through the walls, slab and ceiling were recorded in conjunction with the internal air temperature and relative humidity. Approximately 105 data channels were scanned and logged every 10 min for each of the modules all year round.

The method is very interesting but the data logging period of one month seems to be very large for an energy auditor to measure the thermal properties of a wall.

Biddulph, et al. [16] stated that in-situ monitoring using thermometers and heat flux plates should be carried out in winter over a two-week period to significantly reduce the dynamic effects of the wall's thermal mass from the data.

In this paper, a new methodology is proposed to determine the equivalent thermal properties of a wall by using an advanced thermal calculation method with the least amount of data possible. For this purpose, three parameters should be measured with a constant time step: the temperatures of the inner and outer surfaces of the concerned wall and the heat flux through one of its surfaces (preferably the external surface which generally undergoes more changes over time). One original aspect in the approach is that minimum measurement time can be verified during data acquisition.

2. Methodology

The method is based on the comparison of measured and theoretical heat fluxes and is summarized in Fig. 1. The input

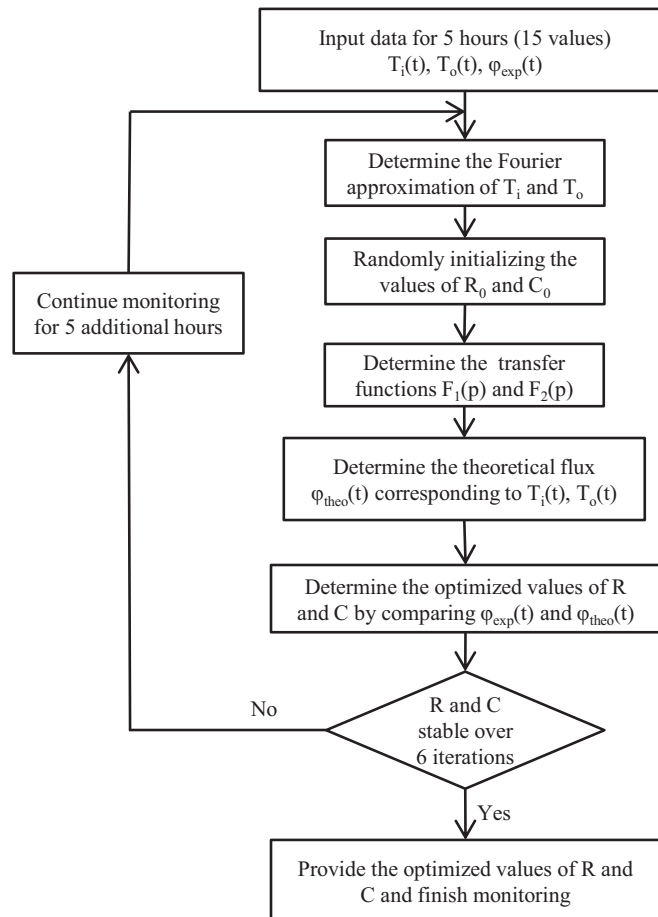


Fig. 1. Process diagram for the proposed method.

data are the temperatures of the inside and outside surfaces of the wall and the outside heat flux.

As explained in the experimental model description, the temperature and heat flux data were recorded at regular time intervals of 20 min, thus, a 5 h monitoring is equivalent to 15 time steps.

The temperatures are decomposed into Fourier series and then used to determine the theoretical heat flux using the matrix of heat transfer for one-dimensional homogeneous multilayer plane constructions in Laplace domain. The elements of the transmission matrices depends on the values of the equivalent thermal resistance R and the equivalent thermal capacity C which initial values are determined randomly and then optimized by comparing the theoretical and experimental heat fluxes by using the least squares method [8]. The optimal values of R and C are confirmed when the relative deviation converges to zero for six consecutive values.

2.1. Mathematical model

The method to deduce the transmission matrix of heat transfer for one-dimensional homogeneous multilayer plane constructions in Laplace domain has been presented in many literatures [17–22]. The deduction process implemented in this study is briefed as follows.

The transmission Eq. (1), in terms of Laplace variable p given in hyperbolic function forms, relates the temperatures and heat flows at both sides of the wall.

$$\begin{bmatrix} T_o \\ \phi_o \end{bmatrix} = \begin{bmatrix} ch(\sqrt{pRC}) & \sqrt{\frac{R}{pC}} sh(\sqrt{pRC}) \\ \sqrt{\frac{pC}{R}} sh(\sqrt{pRC}) & ch(\sqrt{pRC}) \end{bmatrix} \times \begin{bmatrix} T_i \\ \phi_i \end{bmatrix} \quad (1)$$

The Taylor expansion for the elements of the above matrix W_{ij} to the fourth order gives:

$$W_{11}(p) = W_{22}(p) = 1 + \frac{pRC}{2!} + \frac{(pRC)^2}{4!} + \frac{(pRC)^3}{6!} + \frac{(pRC)^4}{8!} \quad (2)$$

$$W_{12}(p) = R \cdot \left[1 + \frac{pRC}{3!} + \frac{(pRC)^2}{5!} + \frac{(pRC)^3}{7!} + \frac{(pRC)^4}{9!} \right] \quad (3)$$

$$W_{21}(p) = pC \cdot \left[1 + \frac{pRC}{3!} + \frac{(pRC)^2}{5!} + \frac{(pRC)^3}{7!} \right] \quad (4)$$

The internal flux is then given by:

$$\phi_i = \frac{T_o - W_{11}T_i}{W_{12}} = F_1(p) \cdot T_i + F_2(p) \cdot T_o \quad (5)$$

The transfer functions $F_1(p)$ and $F_2(p)$ are of the form:

$$F_1(p) = \frac{\alpha p^4 + \beta p^3 + \gamma p^2 + \epsilon p + \mu}{p^4 + ap^3 + bp^2 + cp + d} \quad (6)$$

$$F_2(p) = \frac{\mu}{p^4 + ap^3 + bp^2 + cp + d} \quad (7)$$

The denominator of $F_1(p)$ and $F_2(p)$ can be written [23]:

$$(p - p_1) \cdot (p - p_2) \cdot (p^2 + p_3 \cdot p + p_4) \quad (8)$$

We will present the general solution of $F_1(p)$ since $F_2(p)$ is then a particular case of $F_1(p)$ with $\alpha = \beta = \gamma = \epsilon = 0$. By using the measured data of T_i and T_o it is possible to determine a theoretical internal heat flux $\phi_{i, \text{theo}}$ and then compare it with the measured flux $\phi_{i, \text{meas}}$ then optimize R and C until the difference between the two fluxes is minimal.

T_i and T_o can be decomposed to a finite sum of harmonic signals:

$$T(t) = T_0 + \sum_{n=1}^N [T_{cn} \cos(n\omega t) + T_{sn} \sin(n\omega t)] ; \quad \omega = \frac{2\pi}{D} \quad (9)$$

$$T_0 = \frac{\sum T_i}{D}$$

$$T_{cn} = \frac{2 \cdot \sum [T_k \cos(n\omega t_k)]}{n}$$

$$T_{sn} = \frac{2 \cdot \sum [T_k \sin(n\omega t_k)]}{n} \quad (10)$$

Response to constant excitation T_{cte} :

$$T(t) = cte \Rightarrow T(p) = \frac{T_{cte}}{p} \quad (11)$$

$$\begin{aligned} \phi(p) &= T_{cte} \frac{\alpha p^4 + \beta p^3 + \gamma p^2 + \varepsilon p + \mu}{p \cdot (p^4 + ap^3 + bp^2 + cp + d)} \\ &= T_{cte} \left[\frac{A}{p} + \frac{B}{p - p_1} + \frac{C}{p - p_2} + \frac{Dp + E}{p^2 + p_3p + p_4} \right] \end{aligned} \quad (12)$$

$$\phi(t) = T_{cte} \cdot \left[\begin{aligned} &A + B \cdot \exp(-p_1 t) + C \cdot \exp(-p_2 t) \\ &+ D \cdot \exp\left(\frac{-p_3 t}{2}\right) \cdot \cos(\Omega t) \\ &+ \left(E - \frac{Dp_3}{2}\right) \cdot \exp\left(\frac{-p_3 t}{2}\right) \cdot \sin(\Omega t) \end{aligned} \right]$$

$$\Omega = \sqrt{p_4 - \frac{p_3^2}{4}} \quad (13)$$

Response to sine excitations (T_{sn}):

$$T_{sn}(t) = T_{sn} \cdot \sin(\omega t) \Rightarrow T_{sn}(p) = \frac{T_{sn} \cdot \omega}{p^2 + \omega^2} \quad (14)$$

$$\begin{aligned} \phi(p) &= T_{sn} \frac{\alpha \omega p^4 + \beta \omega p^3 + \gamma \omega p^2 + \varepsilon \omega p + \mu \omega}{(p^2 + \omega^2) \cdot (p^4 + ap^3 + bp^2 + cp + d)} \\ &= T_{sn} \left[\frac{Ap + B}{p^2 + \omega^2} + \frac{C}{p - p_1} + \frac{D}{p - p_2} + \frac{Ep + F}{p^2 + p_3p + p_4} \right] \end{aligned} \quad (15)$$

Response to cosine excitations (T_{cn}):

$$T_{cn}(t) = T_{cn} \cdot \cos(\omega t) \Rightarrow T_{cn}(p) = \frac{T_{cn} \cdot p}{p^2 + \omega^2} \quad (16)$$

$$\begin{aligned} \phi(p) &= T_{cn} \frac{\alpha p^5 + \beta p^4 + \gamma p^3 + \varepsilon p^2 + \mu p}{(p^2 + \omega^2) \cdot (p^4 + ap^3 + bp^2 + cp + d)} \\ &= T_{cn} \left[\frac{Ap + B}{p^2 + \omega^2} + \frac{C}{p - p_1} + \frac{D}{p - p_2} + \frac{Ep + F}{p^2 + p_3p + p_4} \right] \end{aligned} \quad (17)$$

In both cases (sine and cosine excitations), the heat flux is given by:



Fig. 2. Experimental setup of the wall and the heating box.

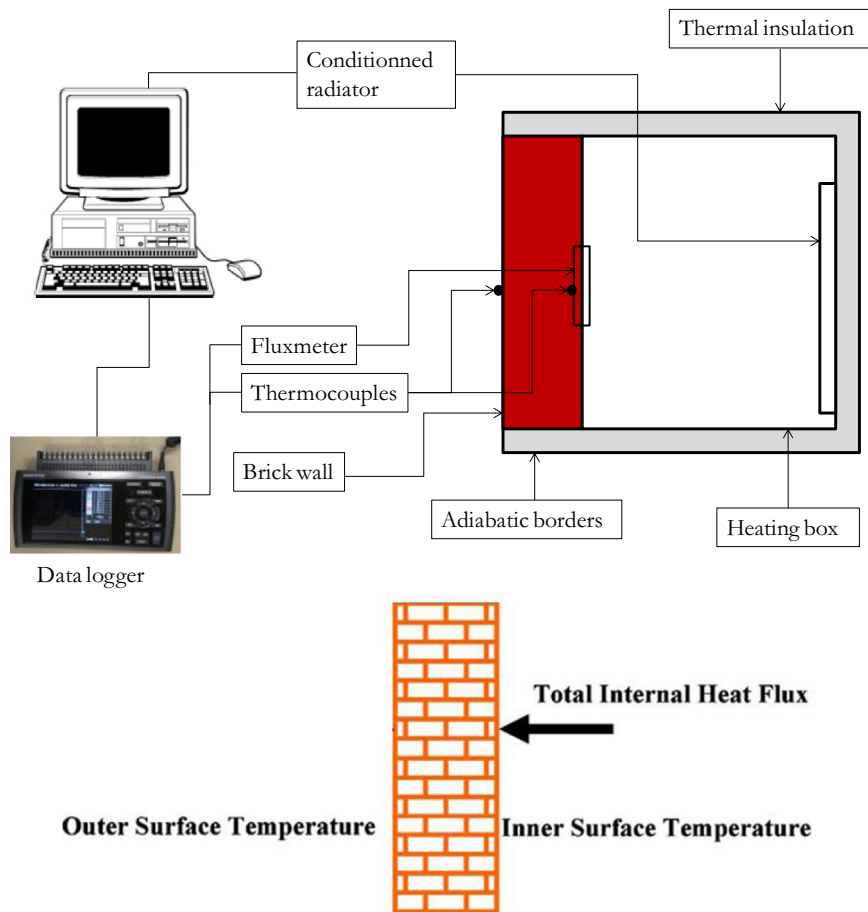


Fig. 3. Schematic cross section of the experimental setup.

$$\phi(t) = T_n \cdot \left[\begin{array}{l} A \cdot \cos(\omega t) + \frac{B}{\omega} \cdot \sin(\omega t) + C \cdot \exp(-p_1 t) \\ + D \cdot \exp(-p_2 t) + E \cdot \exp\left(\frac{-p_3}{2} t\right) \cdot \cos(\Omega t) \\ + \left(F - \frac{E p_3}{2}\right) \cdot \exp\left(\frac{-p_3}{2} t\right) \cdot \sin(\Omega t) \end{array} \right] \quad (18)$$

A, B, C, D, E and F are constants to be determined from the transfer function by identification.

2.2. Experimental model

The experimental wall constitutes one of the four lateral faces of the heating box which contains a radiator with a controlled temperature fluid. The experimental wall is then subjected to a controlled ambiance through the radiator. Two different signal types were programmed for the temperature of the fluid circulating inside the radiator Fig. 2 shows an image of the experimental device (wall and heating box) before it is assembled, and on cross-sectional scheme of the device and its components.

Two thermocouples give the inside and the outside surface temperature of the wall and one flux meter measures the flux passing through the wall at the inside surface of the heating box (Fig. 3).

In the experimental study, the interior of the box represents the external environment of the house, which varies randomly, and the atmosphere of the laboratory (outside the box) represents the interior ambiance of the house where the temperature remains almost constant near 20 °C.

The temperature and heat flux data were recorded at regular time intervals of 20 min through a data logger.

The total experiment data logging duration is approximately 140 h.

The thermal properties of the experimental wall were determined experimentally in steady state laboratory conditions before starting the tests for R and harmonic boundary conditions for C: $R_w = 0,384 \text{ m}^2\text{K/W}$, $C_w = 129,7 \text{ Wh/m}^2\text{K}$.

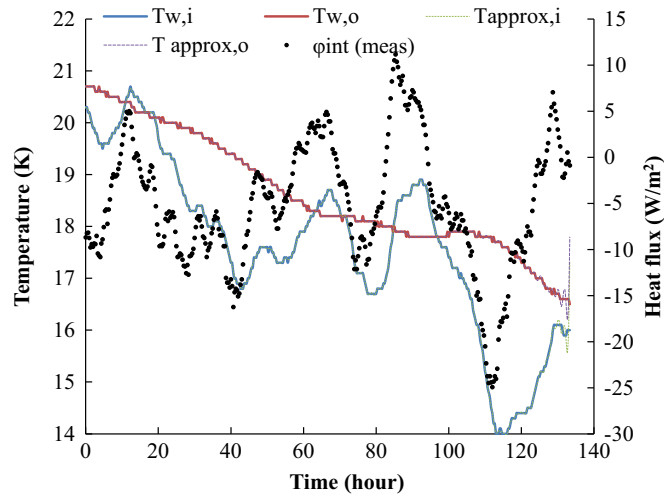


Fig. 4. Input data of the surface temperatures (with their Fourier interpolations) and internal heat flux.

2.3. Optimization process

This optimization process is made through the inverse method [8] by comparing experimental data with the theoretical model meant to describe these data using the least squares method.

After the determination of the theoretical heat flux for random initial values of R and C , the method of least squares is used to minimize the sum of deviations between the measured and calculated heat flux in order to find the optimal values of R and C . The initial values of R and C were chosen randomly ($R_i = 0.6 \text{ m}^2\text{K}/\text{W}$, $C_i = 100 \text{ Wh}/\text{m}^2\text{K}$).

The optimization was performed using the Generalized Reduced Gradient (GRG2) Algorithm which is normally used for optimizing nonlinear problems [24].

3. Results

In Fig. 4, the black dotted curve represents the measured heat flux, the blue line represents the internal wall surface temperature T_i and the green dashed line its corresponding Fourier approximation, the red line represents the internal wall surface temperature T_o and the purple long-dashed line its corresponding Fourier approximation.

Note that the temperature curves and their corresponding approximations are perfectly coincident since the Fourier approximation was developed to the 100th harmonic order ($n=100$).

One of the advantages of this method is that it allows the visualization of heat fluxes generated by the temperatures of the interior and exterior surfaces separately as shown in Fig. 5, which is impossible when it comes to an experimental measurement since the measurement directly gives the total flux at the surface studied. The generated internal flux caused by the external surface temperature (when the internal surface temperature effect is

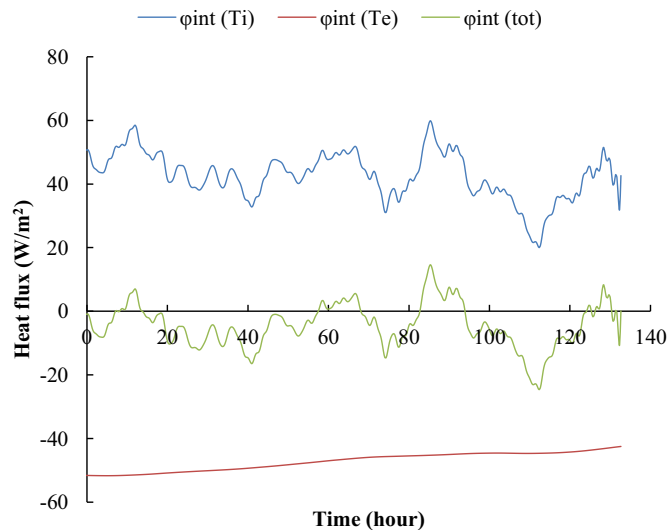


Fig. 5. Numerical heat fluxes generated by internal and external wall surfaces temperatures and total heat flux.

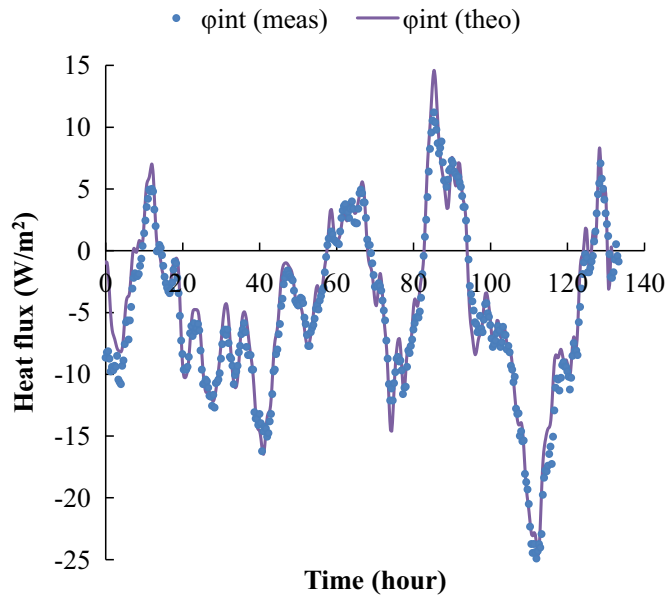


Fig. 6. Comparison between measured and calculated heat flux for the optimized values of R and C.

neglected) is almost constant, this is mainly due to the high capacity of the massive wall studied.

3.1. Determination of R and C

Fig. 6 shows a good accuracy between the measured and calculated heat flux for the optimized values of R and C.

The difference between the theoretical and the measured heat flux is minimal for $R_w=0.400 \text{ m}^2\text{K/W}$ and $C_w=125.5 \text{ Wh/m}^2\text{K}$. For these values, the two curves are very similar which confirms the validity of the method and the obtained results. In addition, the values of R and C are very close to those obtained in steady state boundary conditions with respective relative deviations of 3,9% for R and 3,2% for C.

Note that R and C are equivalent thermal properties of the wall, that means that for multilayered walls they represent the thermal properties of an equivalent homogeneous wall having the same thermal behavior. For an energy engineer or an energy auditor, equivalent R and C are necessary and sufficient, since the main purpose is to determine the thermal behavior of the whole wall and not to identify the physical properties of each of the layers composing it.

3.2. Influence of the monitoring duration on the optimized values of R and C

It is important to determine the minimal measurement time needed to determine R and C without losing too much precision.

For this purpose R and C were determined each 5 h of data record using the cumulated recorded data in order to visualize the convergence of R and C throughout the data logging time.

Fig. 7 shows the variation of the optimal values of R and C throughout the data logging time; it also shows that the 2 curves have similar shapes and

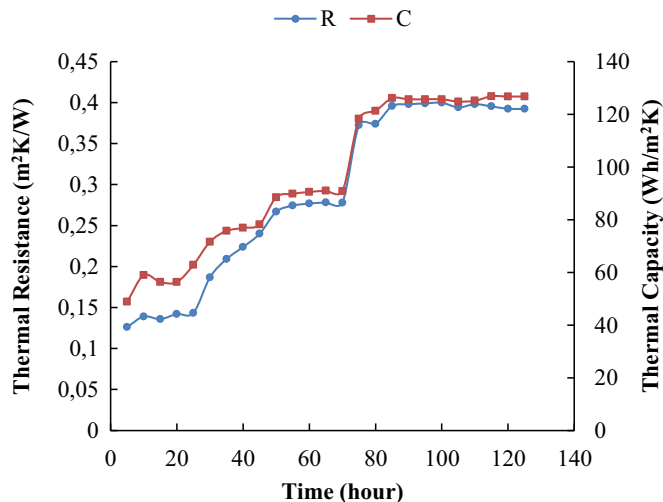


Fig. 7. Variation of the optimal value of R and C throughout the data logging time.

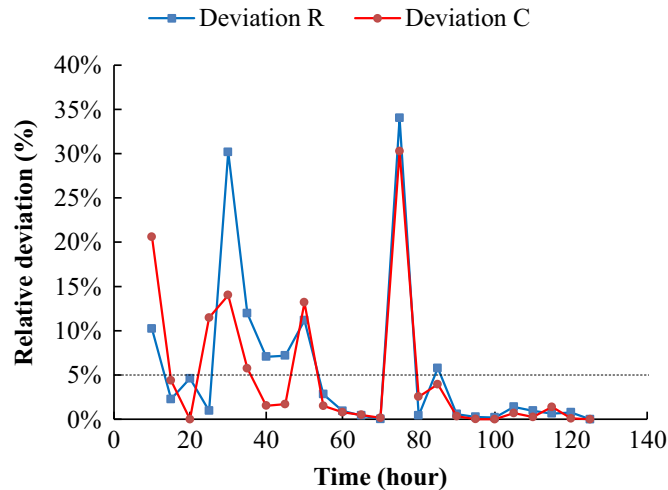


Fig. 8. Relative deviation between 2 consecutive optimal values for R and C.

converge after almost 90 h of data logging (~ four days). However, to ensure that these parameters converge, one additional day of data logging is needed reaching with that around five days of data logging.

This result is in compliance with the results of Ahmad et al. [14] who found that a monitoring period of six days is sufficient to ascertain the in situ thermal transmittance and thermal resistance of reinforced precast concrete walls.

Fig. 8 also shows the same result when comparing two consecutive optimal values for R and C, the relative deviations for both parameters converge to 0 after also after almost 90 h of data logging.

The application of the presented method allows the auditor performing the measurements to check throughout data logging if a convergence is reached.

4. Conclusion and recommendations

This paper offered a practical methodology for thermal characterization of existing walls with a good accuracy. Although the monitoring is relatively long lasting (around 5 days for the case studied), this method remains unsophisticated from an experimental point of view since it doesn't require any imposition of particular boundary conditions and it provides satisfactory and accurate results. By adopting this approach, an energy auditor can now determine the building's walls properties without resorting to personal estimates and assumptions often leading to erroneous studies.

This study described the method adopted which has been proven through measurements in the laboratory; it will be complemented by in-situ tests on various walls under various climate conditions in the upcoming works in order to compare data logging durations needed for different types of existing walls.

References

- [1] V.S.K.V. Harish, Arun Kumar, A review on modeling and simulation of building energy systems, *Renew. Sustain. Energy Rev.* 56 (2016) 1272–1292.
- [2] Rosa Mattia De, Vincenzo Bianco, Federico Scarpa, Luca A. Tagliafico, et al., Heating and cooling building energy demand evaluation; a simplified model and a modified degree days approach, *Appl. Energy* 128 (2014) 217–229.
- [3] Abderrazak Hadded, Sofien Bentoufa, Faten Fayala, Abdelmajid Jemni, et al., Thermo physical characterisation of recycled textile materials used for building insulating Mar, *J. Build. Eng.* 5 (2016) 34–40.
- [4] Fgaier Faycal El, Zoubeir Lafhaj, Emmanuel Antczak, Christophe Chapiseau, et al., Dynamic thermal performance of three types of unfired earth bricks, *Appl. Therm. Eng.* 93 (2016) 377–383.
- [5] Lihua Zhu, Jun Dai, Guoliang Bai, Fengjian Zhang, et al., Study on thermal properties of recycled aggregate concrete and recycled concrete blocks sep, *Constr. Build. Mater.* 94 (2015) 620–628.
- [6] N. Laaroussi, G. Lauriat, M. Garoum, A. Cherki, Y. Jannot, et al., Measurement of thermal properties of brick materials based on clay mixtures nov, *Constr. Build. Mater.* 70 (2014) 351–361.
- [7] R. Derbal, D. Defer, A. Chauchois, E. Antczak, et al., A simple method for building materials thermophysical properties estimation jul, *Constr. Build. Mater.* 63 (2014) 197–205.
- [8] Khaled Chaffar, Alexis Chauchois, Didier Defer, Laurent Zalewski, et al., Thermal characterization of homogeneous walls using inverse method aug, *Energy Build.* 78 (2014) 248–255.
- [9] G. Cattarin, F. Causone, A. Kindinis, L. Pagliano, et al., Outdoor test cells for building envelope experimental characterisation. A literature review, *Renew. Sustain. Energy Rev.* 54 (2016) 606–625.
- [10] Hadia Awad, Mustafa Gül, Hamid Zaman, Haitao Yu, Mohamed Al-Hussein, et al., Evaluation of the thermal and structural performance of potential energy efficient wall systems for mid-rise wood-frame buildings oct, *Energy Build.* 82 (2014) 416–427.
- [11] Asdrubali Francesco, Francesco D'Alessandro, Giorgio Baldinelli, Francesco Bianchi, et al., Evaluating in situ thermal transmittance of green buildings masonries. A case study, *Case Stud. Constr. Mater.* 1 (2014) 53–59.
- [12] Ficco Giorgio, Fabio Iannetta, Elvira Ianniello, Francesca Romana d'Ambrosio Alfano, Marco Dell'Isola, et al., U-value in situ measurement for energy diagnosis of existing buildings oct, *Energy Build.* 104 (2015) 108–121.

- [13] Xi Meng, Biao Yan, Yanna Gao, Jun Wang, Wei Zhang, Enshen Long, et al., Factors affecting the in situ measurement accuracy of the wall heat transfer coefficient using the heat flow meter method, *Energy Build.* 86 (2015) 754–765.
- [14] Aftab Ahmad, Mohammed Maslehuddin, Luai M. Al-Hadhrami, et al., In situ measurement of thermal transmittance and thermal resistance of hollow reinforced precast concrete walls, *Energy Build.* 84 (2014) 132–141. dec.
- [15] C. Luo, B. Moghtaderi, S. Hands, A. Page, Determining the thermal capacitance, conductivity and the convective heat transfer coefficient of a brick wall by annually monitored temperatures and total heat fluxes, *Energy Build.* 43 (2010) 379–385.
- [16] Phillip Biddulph, et al., Inferring the thermal resistance and effective thermal mass of a wall using frequent temperature and heat flux measurements, *Energy Build.* 78 (2014) 10–16.
- [17] G. Fraisse, C. Viardot, O. Lafabrie, G. Achard, Development of a simplified and accurate building model based on electrical analogy, *Energy Build.* 34 (10) (. 2002) 1017–1031.
- [18] P. Lagonotte, Y. Bertin, J.B. Saulnier, Analyse de la qualité de modèles nodaux réduits à l'aide de la méthode des quadripôles, *Int. J. Therm. Sci.* 38 (1999) 51–65.
- [19] NF. EN. ISO13786, Performance thermique d'ES COMPOSANTS DE BÂTIMENT - Caractéristiques thermiques dynamiques - Méthodes de CALCUL, 2008.
- [20] J.-J. Roux, Proposition de modèles simplifiés pour l'étude du comportement thermique des bâtiments, INSA, Lyon, 1984.
- [21] X. Xu, S. Wang, A simplified dynamic model for existing buildings using CTF and thermal network models, *Int. J. Therm. Sci.* 47 (9) (2008) 1249–1262.
- [22] A. Gasparella, G. Pernigotto, M. Baratieri, P. Baggio, Thermal dynamic transfer properties of the opaque envelope: analytical and numerical tools for the assessment of the response to summer outdoor conditions, *Energy Build.* 43 (9) (2011) 2509–2517.
- [23] Polynômes et racines. Christophe Ritzenthaler, 2012.
- [24] L. Lasdon, Large scale nonlinear programming, *Comput. Chem. Eng.* 7 (5) (1983) 595–604.